Journal of Cellular Biochemistry 74:323–333 (1999)

Three-Dimensional Model of the Ligand Binding Domain of the Nuclear Receptor for 1α,25-Dihydroxy-Vitamin D_3

Anthony W. Norman,[1]* Derk Adams,[2] Elaine D. Collins,[1] William H. Okamura,[3] and Robert J. Fletterick[4]

[1]Department of Biochemistry, University of California—Riverside, Riverside, California 92521
[2]Center for Visual Computing, University of California—Riverside, Riverside, California 92521
[3]Department of Chemistry, University of California—Riverside, Riverside, California 92521
[4]Department of Biochemistry and Biophysics, University of California—San Francisco, San Francisco, California 94143

Abstract A three-dimensional model for residues 142–427 of the ligand binding domain (LBD) of the human nuclear receptor for 1α,25-dihydroxy-vitamin D_3 [VDR] has been generated based on the X-ray crystallographic atomic coordinates of the LBD of the rat α1 thyroid receptor (TR). The VDR LBD model is an elongated globular shape comprised of an antiparallel α-helical triple sandwich topology, made up of 12 α-helical elements linked by short loop structures; collectively these structural features are similar to the characteristic secondary and tertiary structures for six nuclear receptors with known X-ray structures. The model has been used to describe the interaction of the conformationally flexible natural hormone, 1α,25-dihydroxy-vitamin D_3 [1α,25$(OH)_2D_3$], and a number of related analogs with the VDR LBD. The optimal orientation of the 1α,25$(OH)_2D_3$ in the LBD is with its A-ring directed towards the interior and its flexible side chain pointing towards and interacting with helix-12, site of the activation function-2 domain (AF-2) of the VDR. Mapping of four natural and one experimental point mutations of the VDR LBD, which result in ligand-related receptor dysfunction, indicates the close proximity of these amino acids to the bound ligand. J. Cell. Biochem. 74:323–333, 1999.

Key words: 1α,25$(OH)_2D_3$; nuclear receptor; steroid receptor; model

The biological actions of the vitamin D receptor (VDR), like those of other nuclear receptors, are dependent upon its interaction with a functionally active ligand; in the case of the VDR, the ligand is the steroid hormone 1α,25-dihydroxy-vitamin D_3 [1α,25$(OH)_2D_3$]. The binding of ligands to nuclear receptors, including the VDR, leads to conformational changes in the receptor [Peleg et al., 1995], that promote formation of heterodimers with the retinoid X receptor (RXR) [Whitfield et al., 1995] and enhance binding to DNA [Freedman, Towers, 1991], coactivators [Hong et al., 1997; Baudino et al., 1998], and transcriptional activation [Rachez et al., 1998].

Grant sponsor: USPHS; Grant number: DK-09012-34.

Elaine D. Collins is currently at the Department of Chemistry, San Jose State University, San Jose, CA 95192.

*Correspondence to: Anthony W. Norman, Department of Biochemistry, University of California, Riverside, CA 92521. E-mail: Norman@ucrac1.ucr.edu.

Received 9 April 1999; Accepted 12 April 1999

We have recently reviewed the scientific literature concerning 278 analogs of 1α,25$(OH)_2D_3$ known to interact as a ligand with the VDR [Bouillon et al., 1995]. While the effect of ligand structural changes has been well studied with regard to receptor binding and ability to effect stimulation of gene transcription, there is not yet available any detailed structural insight into the nature of the ligand binding domain (LBD) of the VDR protein.

In contrast, there is now detailed information derived from determination of the X-ray crystallographic structures of the nuclear receptor LBD for six other hormones. These include the thyroid hormone receptor (TR) [Wagner et al., 1995], the retinoic acid receptor (RARγ) [Renaud et al., 1995], the estrogen receptor (ER) [Brzozowski et al., 1997; Tanenbaum et al., 1998], the progesterone receptor [Tanenbaum et al., 1998], and the ligand binding and coactivator assembly of the peroxisome proliferator-activated-receptor (PPARγ) [Nolte et al.,

1998]; these structures have all been determined with their respective bound ligands. For the ER LBD, an X-ray structure is also known with the bound ligand raloxifene, a tissue specific antagonist of the transcriptional activation function of the ligand-receptor complex [Brzozowski et al., 1997]. Also, the X-ray structure is known for the LBD of the unoccupied 9-*cis* retinoic acid receptor (RXRα) [Bourguet et al., 1995]. All six receptor protein LBDs are found to be remarkably similar with respect to their basic secondary and tertiary structural elements.

The purpose of this communication is to describe the generation of a three dimensional model for the VDR LBD based on the X-ray crystallographic structure of the TR LBD. This VDR model is then evaluated with respect to a number of ligand-receptor structure function topics.

MATERIALS AND METHODS

The model of the LBD of the nuclear receptor for $1\alpha,25(OH)_2D_3$ was generated using the Insight II molecular modeling program (version 6.0). For the human VDR LBD, residues 142–427 were manually aligned with residues 157–410 of the rat α1 isoform of the TR. After the optimal alignment was determined, the atomic coordinates of TR, obtained from its 2.0 Å X-ray crystallographic structure [Wagner et al., 1995], were applied to the aligned VDR residues. The resulting model of the VDR LBD (without ligand) was then conservatively adjusted by energy minimization to a root mean square (RMS) of 0.21. This allowed the model to be subjected to 20,000 iterations of dynamics (300°K) to define our working VDR LBD model. Subsequently $1\alpha,25(OH)_2D_3$ was docked in the VDR LBD and an additional 15,000 iterations of dynamics (300°K) were run.

RESULTS AND DISCUSSION

The iterative approach for defining alignment(s) of the VDR LBD with the TR LBD was based on both the suggestion of a canonical structure for the LBD of nuclear receptors [Wurtz et al., 1996] and comparison of the TR [Wagner et al., 1995] and RARγ [Renaud et al., 1995] X-ray structures which have a highly similar common fold. Three different VDR/TR alignments were originally generated and compared using the Insight Homology program. Although scheme A (not shown), achieved an exact alignment of 90 identical residues between the VDR and TR, it resulted in the arbitrary presence of 25 breaks in the VDR sequence; accordingly alignment A was rejected. Schemes B (Fig. 1) and C (not shown) had identical alignments from VDR residue L224 and TR residue L212 to their respective carboxy terminus, but differed in the size of a VDR loop (either 25 or 42 amino acids) which is positioned between helices 2 and 3. Alignment B was chosen over alignment C based on a greater number of identical (58 vs. 54) and conserved (75 vs. 70) residues between the VDR and TR, a smaller number of unassigned TR residue coordinates (10 vs. 12) and a smaller number of VDR residues without 'assigned' coordinates (42 vs. 54).

Figure 1 presents the selected alignment B of the LBD of the VDR with the TR which was used to generate the three dimensional model of the VDR LBD. It describes only the ligand binding domain of the VDR from residues T142 to the carboxy terminal S427 and includes a loop of 25 residues from S199 to Q223 that could not be included in the alignment with the TR.

The resulting VDR LBD model with $1\alpha,25(OH)_2D_3$ as the docked ligand is shown in Figure 2A and C. The VDR protein model is an elongated globular shape comprised of an antiparallel helical triple sandwich topology, made up of 12 α-helical elements linked by short loop structures; collectively these structural features are similar to the characteristic secondary and tertiary structures of the six nuclear receptors with known X-ray crystal structures. Since prolines are not normally found in α-helices, the presence of the P155, P156 doublet in the VDR suggests that helix 1 will be nonlinear. With respect to the VDR 'loop' region [S199–Q223], it was not possible to identify any secondary structure nor was there any sequence homology with domains on other proteins. The volume of the $1\alpha,25(OH)_2D_3$ ligand is $\approx$375 Å^3 while that of the VDR LBD cavity available to the ligand is $\approx$620 Å^3.

The molecule vitamin D_3 and all its metabolites, including the steroid hormone $1\alpha,25(OH)_2D_3$, are, in comparison to other steroid hormones, unusually conformationally flexible; see Figure 3 for a detailed discussion. The issues regarding selection of the appropriate conformational shape of the $1\alpha,25(OH)_2D_3$ molecule to be docked into the LBD of the VDR are described in detail

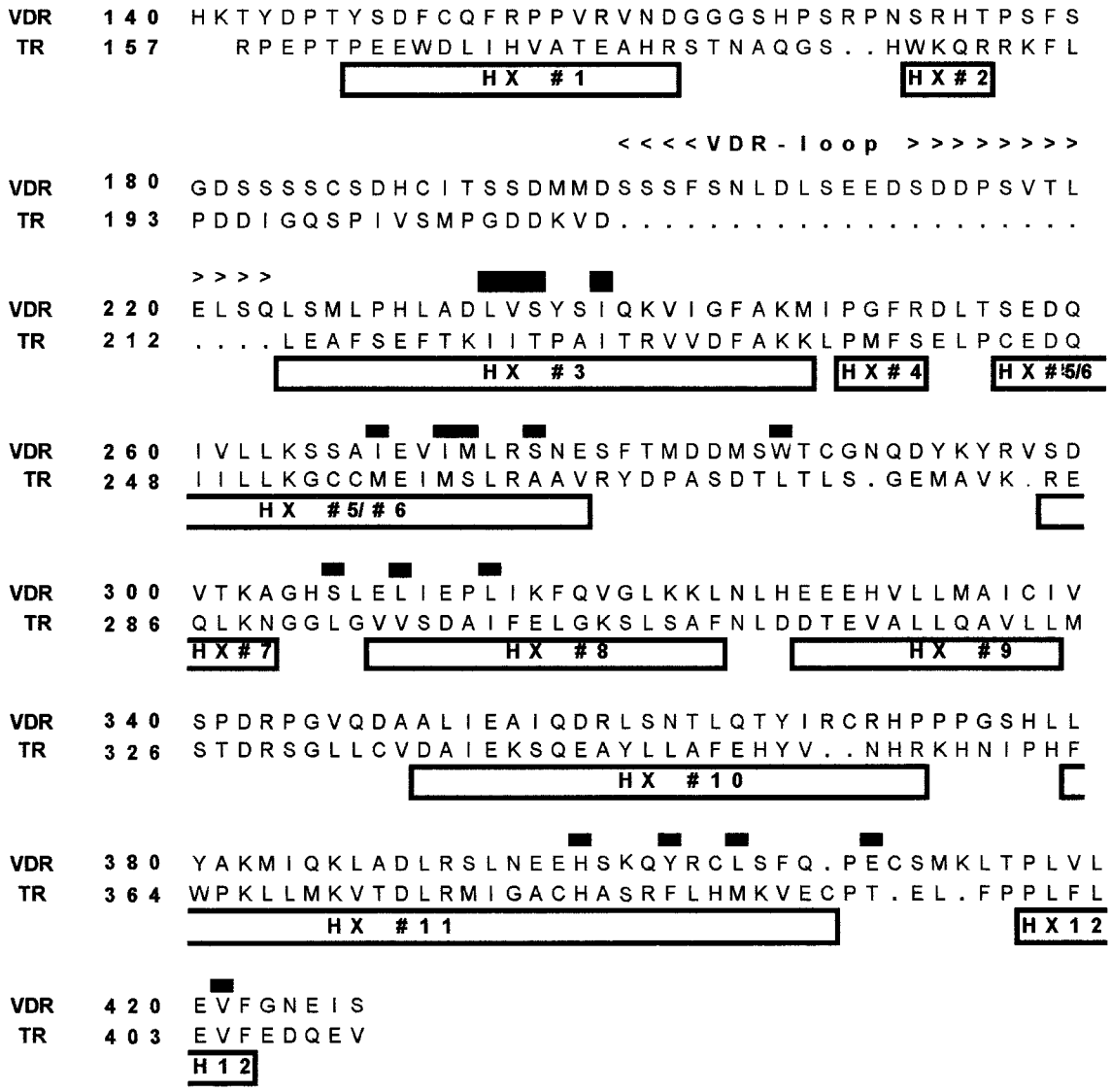

Fig. 1. Alignment of a portion of the VDR LBD with the TR LBD. The amino acid sequence of the human VDR considered in this paper extends from residues 142 to 427. It describes only the ligand binding domain of the VDR including a loop of 25 residues from S199 to Q223 that could not be included in the alignment with the TR. The amino acid sequence of the rat α1 TR structure that was used extends from residues 157 to 410 and describes only the TR LBD [Wagner et al., 1995]. The closed boxes indicate the position of the 12 α-helices that are defined by the TR X-ray structure [Wagner et al., 1995]. The solid bars above the VDR sequence correspond to amino acid residues in the VDR which make close contact (3–4 Å) with a portion of the docked 1α,25$(OH)_2D_3$ (see Fig. 2A).

in the legend to Figure 2 and in later portions of this communication. The direction of orientation of the ligand molecule in the VDR LBD (A-ring inward vs. side chain) was determined by reference to the orientation of ligands in the ER [Brzozowski et al., 1997] and PR [Tanenbaum et al., 1998]. For both receptors, which have classic steroids as ligands, the ligand A-rings were pointed toward the interior of the LBD cavity while the D rings were directed towards helix 12.

The interior surface of the VDR LBD, like the other nuclear steroid receptors, is comprised mostly of hydrophobic residues. The black bars shown in Figure 1 along the VDR sequence identify 16, mostly hydrophobic, residues that are within 3–4 Å of the docked ligand. Evaluation of the interior surface of the LBD for potential hydrogen bond donors for interaction with the three hydroxyl groups of 1α,25$(OH)_2D_3$ indicated a bimodal distribution of hydrophilic residues at the ends of the LBD. Thus, nominee

hydrogen bond donors for the A-ring 1α-OH and 3β-OH groups include S235, S237, and S275, while residues H305, S306, Y401, S405, and T415 are obvious nominees for hydrogen bonding with the side chain 25-OH group. The $1\alpha,25(OH)_2D_3$ ligand shown in Figure 2 has its 1α-OH, 3β-OH, and 25-OH docked near S237, S275, and Y401 of the VDR LBD, respectively. This has the consequence of having the A-ring oriented 'in' towards the interior of the LBD and the side chain oriented 'out' towards helix 12 (the site of the AF-2 domain).

When the four ribbon views of the VDR (Fig. 2A) are converted to CP space-filling views (data not shown), no hint of the ligand is apparent on the VDR surface, nor is there an obvious entrance portal discernable for the ligand. Given the fact that the ligands of all the nuclear receptors are completely buried in the interior of their cognate receptors [Wagner et al., 1995; Renaud et al., 1995; Brzozowski et al., 1997; Williams, Sigler, 1998; Nolte et al., 1998], an intriguing question is: by what route does the ligand gain access to the LBD cavity? One pos-

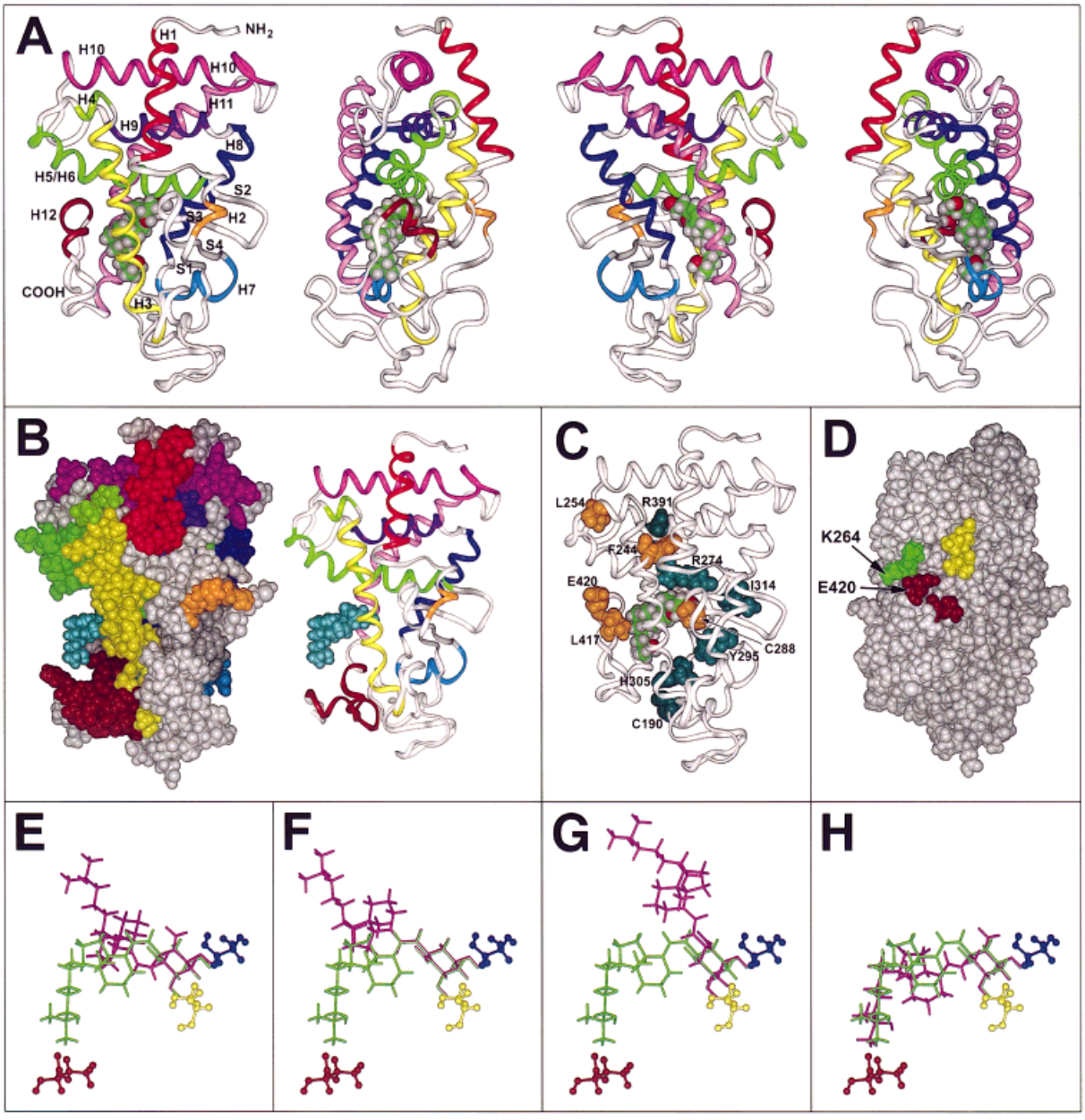

Figure 2.

sible answer has been provided by Renaud et al. [1995]. These authors compared the X-ray structure of the unoccupied RXRα [Bourguet et al., 1995] with the occupied RARγ [Renaud et al., 1995], and noted that the only significant difference was in the different positions of helix 12. As a consequence, they proposed two conformational states for the apo- and holo-LBDs of nuclear receptors [Renaud et al., 1995]. In the unoccupied receptor, helix 12 is rotated out and down to create an open portal, while in the occupied receptor, helix 12 is rotated up to interact with helices 3 and 5 which has the consequence of closing the portal. Figure 2B presents the open portal view of the VDR in both the ribbon and CP space-filling views; this should be contrasted with the closed portal views of the VDR (Fig. 2A,D).

Table 1 summarizes six natural and five experimental mutations in the LBD of the VDR that have identified amino acids critical for normal LBD function. The positions of these mutations in the VDR LBD in relation to the ligand 1α,25$(OH)_2D_3$ are shown in Figure 2C. It is apparent that the natural [R274L, Y295stop, H305Q, I314S] and the experimental [C288G] mutations, which are typified by changes in ligand binding, are all proximal to 1α,25$(OH)_2D_3$. In contrast the C190N, F244G, L254G, R391C, L417A, and E420A mutations, which do not affect ligand binding, but do display either impaired heterodimer formation or transactivation, are located at a greater distance from the 1α,25$(OH)_2D_3$ ligand.

Binding of a ligand by a nuclear receptor confers upon the complex the ability to selectively interact with coactivator proteins to generate a competent transcriptional complex [Glass et al., 1997; Hong et al., 1997]. Recently, site-directed scanning surface mutagenesis of the TR identified six key residues (two each on helices 3, 5, and 12) which contribute to the formation of a specific small hydrophobic cleft on the receptor surface which is essential for binding the glucocorticoid receptor-interacting protein 1 (GRIP1) or steroid receptor coactivator (SRC-1) coactivators [Feng et al., 1998]. Two of the residues, one each on helices 3 and 12, are completely conserved among nuclear receptors, including the VDR (K246, E420) [Wurtz et al., 1996]. Ligand activation of transcription is believed to be achieved by folding the receptor

Fig. 2. Three-dimensional model of the VDR LBD. A–D illustrate different representations of the same three-dimensional model of the VDR LBD. The ligand in A–D is 1α,25$(OH)_2D_3$; its atoms are colored so that hydrogen is grey, oxygen red, and carbon green. The 1α,25$(OH)_2D_3$ is in a conformation close to the planar 6-s-*cis* shape of Fig. 3D. The A-ring is in the chair-conformer-A (Fig. 3B) where the 1α-OH is axial and the 3β-OH is equatorial. The side chain is oriented in its 'northeasterly' or 2 o'clock orientation as defined by its global minimum energy (see Fig. 3B 'dot map' with line tracing of the side chain; [Okamura et al., 1992]). **A:** Four successive 90° rotations around the vertical axis of the VDR model present on the left side. Each view illustrates a different perspective of the 12 α-helices (presented as ribbons) and four β-strands that collectively define the LBD of the VDR. The helices are numbered in the same order (H1–H12) as for the TR [Wagner et al., 1995] structure (see Fig. 1). Each helix has its own unique color that is retained in B and C. The light white loop present at the bottom of the VDR LBD model represents the 25 residues present between helices 2 and 3 termed 'VDR loop' in Figure 1. **B:** 1α,25$(OH)_2D_3$ (blue colored molecule) beginning to enter the VDR LBD. In B, the right side is an α-helix ribbon diagram and the left side is a CP space-filling representation; the color coding of the 12 helices is the same as in A. For both views of B, helix 12 (dark red) has been moved (compare with A) to duplicate its position in the RXRα structure which has an unoccupied LBD [Bourguet et al., 1995]. Thus the position of helix 12 reflects the 'open' portal property of an unoccupied receptor which contrasts with the 'closed' portal position of helix 12 in an occupied receptor (A). **C:** One view (comparable to view of the left A) of the VDR LBD and illustrates the position of the six naturally occurring (colored blue) and five experimental (colored red) mutations; the amino acid residues are shown in a CP space-filling representation. **D:** A putative ligand-dependent GRIP1 coactivator binding site on the surface of the VDR. The two red residues are L417 and E420 (helix 12), the two green residues are I260 and K264 (helix 5), and the two yellow residues are I242 and K246 (helix 3). All residues but I242 are conserved in the TR and several other nuclear receptors [Feng et al., 1998]; the I242 is a conservative substitution for a V230 in the TR. The formation of the GRIP1 coactivator binding site is achieved in the TR by the bringing together of selected regions of helices 3, 5, and 12 which occurs after the receptor has bound an agonist ligand; this GRIP1 site is postulated to be stabilized via a salt bridge between residues K264 (helix 5) and E420 (helix 12). **E–H:** A comparison of the similarities and differences between four pairs of different configurations of the 1α,25$(OH)_2D_3$ molecule which are docked in the VDR LBD. Only three residues of the VDR LBD are illustrated; the two nominee hydrogen bond donors (yellow S237 and blue S275) for the 1α-OH and 3β-OH groups of the ligand, and T415 (dark red) as a hydrogen bond donor for the 25-OH group of 1α,25$(OH)_2D_3$. In each of these four panels the green ligand is 1α,25$(OH)_2$-6-s-*cis*-D_3 with the cyclohexane ring in the conformer A representation (designated A-*cis*). The cyclohexane ring of the green A-*cis* molecule is exactly superimposed with the A-ring chair conformer in each of four different configurations of a magenta colored 1α,25$(OH)_2D_3$ molecule. The magenta ligand in E–H is respectively 1α,25$(OH)_2D_3$ in an upside-down B-*cis* (Fig. 2E), A-*trans* (Fig. 2F), upside-down A-*trans* (Fig. 2G), and an upside-down B-*trans* (Fig. 2H) configuration (see text for additional description).

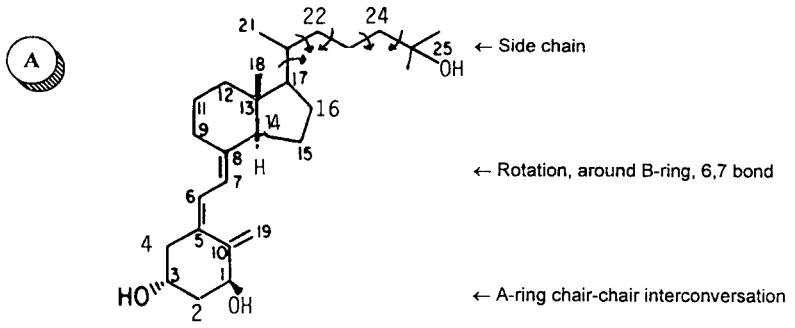

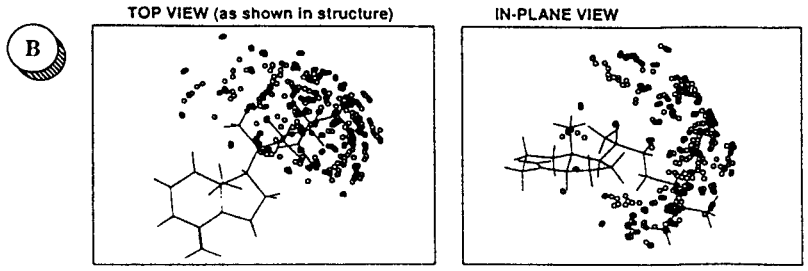

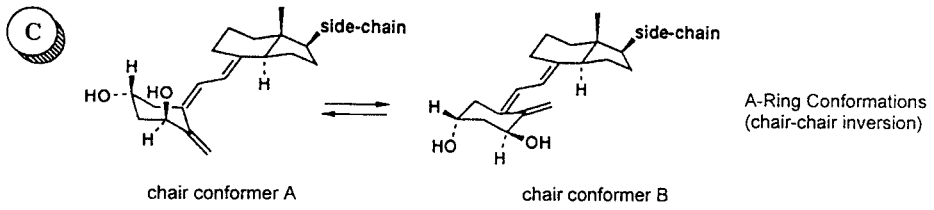

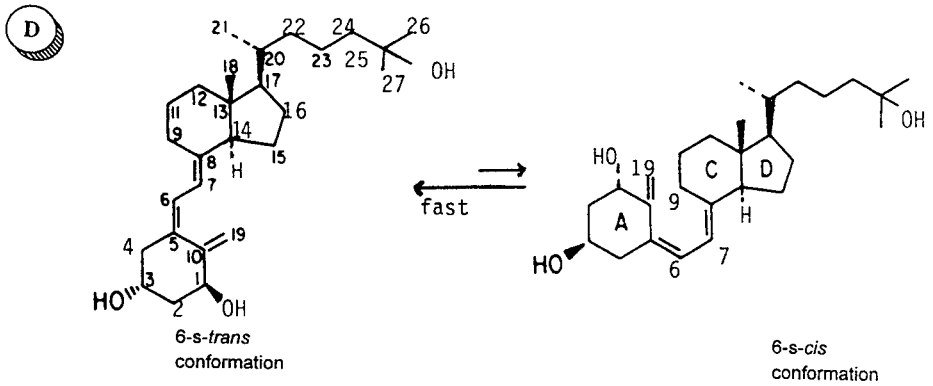

Continuum of 6,7-single bond rotamers of 1,25.

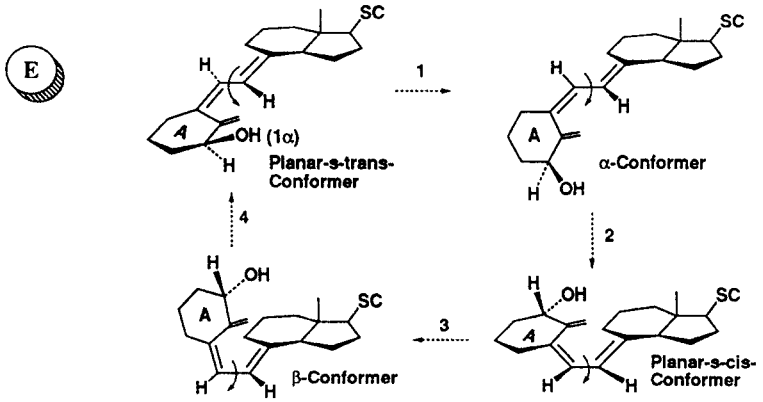

Figure 3.

TABLE I. Summary of Mutations in the LBD of the VDR[a]

Mutation	Consequences	Reference
C190W◆	Familial VDDR-II syndrome	[Thompson et al., 1991]
F244G	Impaired transactivation	[Whitfield et al., 1995]
L254G	Impaired transactivation; No RXR heterodimers	[Whitfield et al., 1995]
R274L◆	Impaired ligand binding; VDRR-II syndrome	[Kristjansson et al., 1993]
C288G	Impaired ligand binding; VDRR-II syndrome	[Nakajima et al., 1996]
Y295 stop◆	Premature termination; no ligand binding	[Ritchie et al., 1989]
H305Q◆	80% decrease in ligand binding and decreased transactivation	[Malloy et al., 1997]
I314S◆	Impaired ligand retention, RXR dimerization and transactivation	[Whitfield et al., 1996]
R391C◆	Impaired RXR dimerization and transactivation	[Whitfield et al., 1996]
L417A	Impaired transactivation	[Jurutka et al., 1997]
E420A	Impaired transactivation	

[a]The mutations are listed sequentially from the amino terminus to the carboxy terminus of the VDR LBD. The symbol ◆ indicates a naturally occurring human mutation. The other mutations were experimental in nature. VDRR-II, vitamin D-dependent rickets, type II.

helix 12 (associated with the AF-2 function) against a scaffold of helices 3–6 to create a small hydrophobic cleft (≈300 Å) on the surface of the receptor that is postulated to match a complementary region on the surface of the coactivator [Feng et al., 1998].

Figure 2D illustrates a putative ligand-dependent GRIP1 coactivator binding site on the surface of the VDR; this representation is quite comparable to Fig. 3B [Feng et al., 1998]. By analogy with the TR, the VDR coactivator binding cleft contains charged and hydrophobic residues at its periphery, but only hydrophobic residues at its center. Residues that are postulated to form the surface cleft include I238, I242, and K246 from helix 3, I260, L263, and K264 from helix 5, A267 from helix 6, and L417, E420, and V421 from helix 12. The formation of the cleft is stabilized by a salt bridge between the two TR/VDR conserved residues, E420 (helix 12) and K264 (helix 5). It is also known (Table I) that mutation of L417A [Jurutka et al., 1997] which is postulated to be involved in formation of the coactivator cleft results in impairment of VDR transactivation. A key feature of the postulated coactivator binding site is that it is formed in response to the receptor binding an agonist ligand which results in a movement of helix 12 from the 'open' portal position (Fig. 2B) to that of the 'closed' portal position of Fig. 2A,2D. It is known that binding of ligand by the VDR does result in clearly detectable conformational changes as evaluated by differences in trypsin sensitivity [Peleg et al., 1995].

An interesting structure-function relationship between the ligand and the VDR LBD relates to determination of the optimal shape(s) of the ligand which facilitates entrance through the portal of the VDR LBD (Fig. 2B) as contrasted with that required for docking of the ligand 1α-OH, 3β-OH, and 25-OH groups with their nominee hydrogen bond partners on the protein. It is possible that the optimal ligand shape for entrance into the VDR LBD could be a 'slim' [1α,25$(OH)_2$-6-s-*trans*-D_3] molecule while the optimal shape for the ultimate docking with nominee hydrogen bond donors could be closer to the classic steroid 'pudgy' [1α,25$(OH)_2$-6-s-*cis*-D_3] shaped molecule. If there are two different optimal shapes of the ligand, this implies that

Fig. 3. Conformational flexibility of vitamin D molecules using 1α,25$(OH)_2D_3$ as an example. **A:** Structure of 1α,25$(OH)_2D_3$ indicating the three structural features of the molecule which confer unusual (in relation to other steroids)conformational flexibility upon the molecule. **B:** The dynamic 360° side chain rotation about the five single carbon-carbon bonds (indicated by the curved arrows in A). The dots indicate the position in three-dimensional space of the 25-hydroxyl group for some 394 readily identifiable side chain conformations that have been determined from energy minimization calculations [Okamura et al., 1992]. The position of the side chain in its minimal energy state is indicated to be in the "northeast" (2 o'clock) orientation by the line tracing of the side chain. **C:** The rapid (thousands of times per second) chair-chair interconversion of the A-ring of the seco steroid which generates the distinct chair conformer A with the 19-methylene "down" (1α-OH axial, 3β-OH equatorial) and chair conformer B with the 19-methylene "up" (1α-OH equatorial, 3β-OH axial). **D:** The rapid 360° rotational freedom about the 6,7 single carbon-carbon bond of the seco B ring which generates conformations ranging from the more steroid-like (6-s-*cis*) conformation to the open and extended (6-s-*trans*) conformation of 1α,25$(OH)_2D_3$. **E:** Further illustration of the 360° rotation about the 6,7 carbon-carbon bond. Four steps of successive 90° rotations are illustrated. Each intermediate structure has a different shape, particularly with respect to the position of the critical 1α-hydroxyl and the plane of the A-ring in relation to the plane of the C/D-rings.

there must be sufficient volume available in the LBD cavity for the conformationally flexible $1\alpha,25(OH)_2D_3$ to achieve the necessary alterations in its shape.

A description of the many shapes of $1\alpha,25(OH)_2D_3$ which arise because of the conformational flexibility of the A-ring, rotation about the 6,7 carbon single bond and the conformational mobility of the side chain are summarized in Figure 3. Because vitamin D and its daughter metabolites do not have a 9,10 carbon bond (i.e., the B-ring is broken, which is a characteristic of a seco steroid), the cyclohexane A-ring is no longer fused to the B-ring and is free to undergo chair-chair inversion between conformer A and conformer B (Fig. 3C). The principal structural change is the inversion of the 1α-OH/3β-OH pair of the cyclohexane ring from the axial/equatorial (conformer A) to the equatorial/axial (conformer B) orientation; this has the consequence of moving each hydroxyl approximately 3.8 Å, which is enough to disrupt the postulated stabilizing hydrogen bonds between the VDR LBD and ligand.

There are also significant consequences for the $1\alpha,25(OH)_2D_3$ molecule when it undergoes a 180° rotation about the 6,7 carbon single bond (6-s-*cis* conformer vs. 6-s-*trans* conformer; see Fig. 3D). When the chair conformer A of a 6-s-*cis* $1\alpha,25(OH)_2D_3$ molecule is exactly aligned with the chair conformer A of a 6-s-*trans* $1\alpha,25(OH)_2D_3$ molecule, with both side chains in their global minimum position (Fig. 3B), the distance from the 1α-OH to 25-OH increases from 11.7 to 14.7 Å and for the 3β-OH to 25-OH group increases from 9.6 to 14.9 Å in changing from the 6-s-*cis* to 6-s-*trans* orientation. Again these are distance changes capable of disrupting hydrogen bonds between the ligand and VDR LBD.

Given the restricted volume of the interior cavity of the VDR LBD (≈620 $Å^3$ by analogy with TR) in relation to the volume of a $1\alpha,25(OH)_2D_3$ molecule (375 $Å^3$), it is not clear whether there is sufficient room for a $1\alpha,25(OH)_2D_3$ molecule when present in the VDR LBD to carry out the necessary 180° rotation required to convert from the 6-s-*cis* to the 6-s-*trans* orientation. It is more likely, though, that the LBD volume can accommodate the chair conformer A and chair conformer B cyclohexane ring interconversions (Fig. 3C). When evaluating a seco steroid ligand for docking into the VDR LBD, careful consideration should be given to determining which of the two cyclohexane ring chair conformers (A vs. B) and which of the two orientations about the 6,7 single carbon bond (*cis* vs. *trans*) are appropriate for utilization. These four configurations can be designated as A-*cis*, B-*cis*, A-*trans*, and B-*trans*, respectively. Accordingly, four Case studies can be identified for comparison of these four configurations; in each of these the reference shape is that of the molecule in the A-*cis* (chair conformer A of $1\alpha,25[OH]_2$-6-s-*cis*-D_3) configuration. Figure 2E–H illustrate these four comparisons.

Case #1: A-*cis* vs. B-*cis;* Fig. 2E. When an A-*cis* molecule is docked in the VDR LBD, it is apparent that the axial 1α-OH and equatorial 3β-OH groups can be readily positioned close to the VDR nominee hydrogen bond S237/S275 donor pair (Fig. 2A,E). However, it is not possible to achieve the same three-dimensional relationship between the two A-ring hydroxyls and the VDR S237/S275 pair when docking a B-*cis* molecule because of the inversion of orientation of the two 1α-OH and 3β-OH groups to become equatorial and axial, respectively (Fig. 3C). An appropriate relationship of the hydroxyls of B-*cis* with the S237/S275 donor pair can only be achieved by turning the molecule over by rotating it 180° along its long axis. This upside-down orientation of B-*cis* could permit the necessary axial/equatorial orientation of the two A-ring hydroxyl groups with the S237/S275 donor pair so as to mimic that described above for the A-*cis* conformer (Fig. 2E). However, in this upside-down B-*cis* orientation, the 3β-OH is docked with S237 and the 1α-OH with S275 which is the reverse of the docking arrangement for A-*cis*. Also the 10,19 methylene groups of the A-*cis* and upside-down B-*cis* are on opposites sides of the molecules. In addition, the C/D rings are not well aligned and the side chains are widely separated. Thus we conclude that neither the B-*cis* nor the upside-down B-*cis* orientations are likely viable ligands for the VDR.

Case #2: A-*cis* vs. A-*trans;* Fig. 2F. When the A-ring of an A-*cis* molecule is exactly aligned with the A-ring of an A-*trans* molecule (axial 1α-OH and equatorial 3β-OH groups superimposed), it is apparent that the C/D rings of the two molecules do not align and that there is a wide separation of their side chains. This results because of the 180° rotation around the 6,7 bond of the A-*trans* in relation to the A-*cis*. Thus we conclude that this A-*trans* orientation is not a likely viable ligand for the VDR.

Case #3: A-*cis* vs. upside-down A-*trans;* Fig. 2G. When an A-*trans* molecule is turned over by rotating it 180° around its long axis and then the A-ring is superimposed on the A-ring of a molecule in the A-*cis* orientation, neither the 1α-OH nor 3β-OH groups are superimposable (since both molecules are chair conformer A, but rotated 180°) nor are the C/D rings aligned. In addition, the side chains are widely separated. Thus, since the 1α-OH, 3β-OH, and 25-OH groups can not align with the VDR LBD nominee hydrogen bonds, we conclude that this orientation of the A-*trans* orientation of 1α,25$(OH)_2$-6-s-*trans*-D_3 also is not a likely viable ligand for the VDR.

Case #4: A-*cis* vs. B-*trans;* Fig. 2H. When an A-*cis* configuration is compared with a B-*trans* a surprisingly similar alignment of the two ligands can be achieved. While the two C/D rings are not superimposed, they are parallel, and displaced by only 2.4 Å, and the side chains are also approximately parallel. Thus we provisionally conclude that this conformer of 1α,25$(OH)_2$-6-s-*trans*-D_3 (B-*trans*) can be docked with the three nominee hydrogen bond donors for the 1α-OH, 3β-OH, and 25-OH groups (S237, S275, and Y401).

A test of the biological activities of ligands chemically locked in either the 6-s-*cis* or 6-s-*trans* orientation has been determined with respect to their ability to bind to the VDR and to effect transactivation in whole cell assays [Norman et al., 1997]. Ligands that were locked either in the planar-s-*trans* (1α,25$(OH)_2$-tachysterol$_3$) or the planar-s-*cis* (1α,25$(OH)_2$-7-lumisterol$_3$) shapes (see Fig. 3E) were both poor agonists for the VDR (only 0.1–1.0% the activity of the conformationally flexible 1α,25$(OH)_2D_3$). These results suggested that a probable optimal shape of a ligand for the VDR LBD is one where the plane of the A-ring in relation to the C/D ring is at some intermediate angle (0–90°) as depicted by the α-conformer and β-conformer representations of Figure 3E.

One striking ligand-receptor structure-function relationship for 1α,25$(OH)_2D_3$ analogs relates to the chiral center at carbon 20 (see Fig. 3A) of the steroid side chain [Binderup et al., 1991]. The 20-epi analogs are 100–10,000 times more transcriptionally potent than the natural hormone 1α,25$(OH)_2D_3$, even though their affinity for the VDR is not greater [Peleg et al., 1995]. It is also known that the side chain of 20-normal vs. 20-epi analogs of 1α,25$(OH)_2D_3$ is able to access different regions of three-dimensional space around the C/D ring; thus the position of global minimum energy for the 20-normal analogs (1α,25$[OH]_2D_3$) is oriented to the "northeast" [see Fig. 3B] while for 20-epi analogs it is towards the "northwest" [Midland et al., 1993; Yamada et al., 1998].

The seemingly benign structural change of the ligand from a 20-normal to 20-epi 1α,25$(OH)_2D_3$ results in a new conformational change in the VDR (as assessed by trypsin sensitivity) which is believed to reflect an altered orientation of helix 12. Thus a VDR with a 20-epi ligand has an enhanced dimerization with RXR, resulting in increased transactivation of the osteocalcin promoter [Peleg et al., 1995]. Orientation of the 1α,25$(OH)_2D_3$ side chain towards helix 12, rather than towards the interior of the VDR LBD, is supported by biological activity evaluation of five carboxy terminal truncation mutants of the VDR (L390/TGA, E396/TGA, C403/TGA, C410/TGA, and E420/TGA) [Peleg et al., 1995]. Differences in ligand potency between 20-normal and 20-epi analogs were ascribed to multiple and different contact sites of the side chains with the VDR LBD AF-2 domain (helix 12 in Fig. 2A) [Liu et al., 1997].

We have also evaluated the problem of docking in the VDR LBD a unique analog of 1α,25$(OH)_2D_3$ that has a second side chain attached to carbon 20 (Gemini or 21-[3′-hydroxy-3′-methylbutyl]-1α,25$[OH]_2D_3$). Thus Gemini has both a 20-normal and a 20-epi side chain. Gemini binds 40% as well as 1α,25$(OH)_2D_3$ to the VDR, but is 13-fold more potent than 1α,25$(OH)_2D_3$ with respect to transactivation of the osteocalcin promoter. Interestingly, the Gemini occupied VDR LBD displays a trypsin protease sensitivity different from both the 20-normal or 20-epi versions of 1α,25$(OH)_2D_3$ which has been interpreted to be reflective of a unique shape of the holo receptor [Uskokovic et al., 1997]. We conclude that it is not feasible for Gemini to enter through the VDR open portal leading with its two sidechains which, given their conformational flexibility (Fig. 3B), create an improbably large bulk to be readily accommodated. This conclusion is also consistent both with the proposal that the ligand enters the VDR LBD leading with its A-ring and with the unique trypsin sensitivity of a VDR LBD-Gemini complex. This protease sensitivity could reflect the interaction of both Gemini side

chains with helix 12 to generate a unique shape resulting in exceptional transactivation potency in comparison to when the 20-normal $1\alpha,25(OH)_2D_3$ is the ligand.

One of the striking features of VDR LBD is the multiplicity of proposed hydrogen bond donor/acceptors for the side chain of the ligand; these include H305, S306, Y401, S405, and T415. This may be a reflection of the fact that a VDR receptor with multiple docking sites for the 25-OH of the conformationally flexible side chain of $1\alpha,25(OH)_2D_3$ would have an advantage over a VDR receptor with only one docking site for the 25-OH group. It is also interesting that the natural mutation H305Q of VDR has an 80% decreased ligand affinity; this suggests a functional involvement of H305 in some aspect of ligand binding. Possibly H305 is important in the open portal mode of the VDR (Fig. 2B) to stabilize the side chain under circumstances where the three other nominee hydrogen bond donors (Y401, S405, and T415) for the 25-OH group are inaccessible because helix 12 has moved to the open position. Only when helix 12 is closed are these three donors accessible to the 25-OH group.

Two models of the VDR LBD have been previously proposed. Raynaud et al. [1991] constructed a model in 1991 using the structure prediction methodology of hydrophobic cluster analysis to propose a model of the VDR LBD. They made some predictions with regard to identification of possible heterodimerization domains and nuclear localization signals, but little specific information was provided concerning details of ligand receptor interaction. Wurtz et al. [1997], utilizing the X-ray structure of the holo RARγ, proposed a holo VDR LBD model with $1\alpha,25(OH)_2D_3$ as the docked ligand. The basic fold of the Wurtz et al. VDR LBD model was similar to that reported in this communication, which is to be expected given the high structural similarity of the six nuclear hormone receptors with known LBD X-ray structures. There are a number of important differences between the Wurtz et al. model and that presented in Figure 2A. These include the following: (a) the reverse orientation (side chain 'in' and A-ring towards helix 12) of the ligand in the LBD pocket; (b) the 6-s-*trans* rather than the 6-s-*cis* conformer of $1\alpha,25(OH)_2D_3$ for the ligand; and (c) the size of the loop between helices 2 and 3. This difference in loop size is attributable to the alignment of the VDR with RARγ as compared to the alignment with TR (Fig. 1). As yet no natural mutations have been mapped to the loop regions nor has biological significance been attributed to any of the residues associated with either of the loop regions.

The present model of the VDR LBD is useful for visualizing structure-function relationships between the receptor and its natural hormone, $1\alpha,25(OH)_2D_3$, as well as a number of analogs. The potential complexity of the relationships between the VDR and the conformationally flexible ligand $1\alpha,25(OH)_2D_3$ is particularly intriguing and should stimulate aspects of rational drug design. The model has predictive value, so that, for example, it will be possible to carry out site directed mutagenesis of the VDR LBD nominee residues for interacting with the key the 1α-OH, 3β-OH, and 25-OH groups. The current VDR LBD model has facilitated analysis of surface domains, such as that for GRIP1, and is anticipated to be useful for understanding the structural relationships important for heterodimer formation between the VDR and RXRα. However the determination of the X-ray structure of the VDR LBD is still a long awaited essential objective. Only then can the suggestions derived from this model be supported, modified or rejected based on the reality of the determined structure.

ACKNOWLEDGMENTS

The authors greatly benefitted from extensive discussions with Dr. Helen L. Henry concerning the VDR LBD model and the editorial assistance of Ms. June E. Bishop.

REFERENCES

Baudino TA, Kraichely DM, Jefcoat SC, Jr., Winchester SK, Partridge NC, MacDonald PN. 1998. Isolation and characterization of a novel coactivator protein, NCoA-62, involved in vitamin D-mediated transcription. J Biol Chem 273:16434–16441.

Binderup L, Latini S, Binderup E, Bretting C, Calverley M, Hansen K. 1991. 20-Epi-vitamin D_3 analogues: a novel class of potent regulators of cell growth and immune responses. Biochem Pharm 42:1569–1575.

Bouillon R, Okamura WH, Norman AW. 1995. Structure-function relationships in the vitamin D endocrine system. Endocr Rev 16:200–257.

Bourguet W, Ruff M, Chambon P, Gronemeyer H, Moras D. 1995. Crystal structure of the ligand-binding domain of the human nuclear receptor RXR-α. Nature 375:377–382.

Brzozowski AM, Pike ACW, Dauter Z, Hubbard RE, Bonn T, Engstrom O, Ohman L, Greene GL, Gustafsson J-A, Carlquist M. 1997. Molecular basis of agonism and antagonism of the oestrogen receptor. Nature 389:753–757.

Feng WJ, Ribeiro RC, Wagner RL, Nguyen H, Apriletti JW, Fletterick RJ, Baxter JD, Kushner PJ, West BL. 1998. Hormone-dependent coactivator binding to a hydrophobic cleft on nuclear receptors. Science 280:1747–1749.

Freedman LP, Towers TL. 1991. DNA binding properties of the vitamin D_3 receptor zinc finger region. Mol Endocrinol 5:1815–1826.

Glass CK, Rose DW, Rosenfeld MG. 1997. Nuclear receptor coactivators. Curr Opin Cell Biol 9:222–232.

Hong H, Kohli K, Garabedian MJ, Stallcup MR. 1997. GRIP1, a transcriptional coactivator for the AF-2 transactivation domain of steroid, thyroid, retinoid, and vitamin D receptors. Mol Cell Biol 17:2735–2744.

Jurutka PW, Hsieh JC, Remus LS, Whitfield GK, Thompson PD, Haussler CA, Blanco JC, Ozato K, Haussler MR. 1997. Mutations in the 1,25-dihydroxyvitamin D_3 receptor identifying C-terminal amino acids required for transcriptional activation that are functionally dissociated from hormone binding, heterodimeric DNA binding, and interaction with basal transcription factor IIB, in vitro. J Biol Chem 272:14592–14599.

Kristjansson K, Rut AR, Hewison M, O'Riordan JLH, Hughes MR. 1993. Two mutations in the hormone binding domain of the vitamin D receptor cause tissue resistance to 1,25 dihydroxyvitamin D_3. J Clin Invest 92:12–16.

Liu YY, Collins ED, Norman AW, Peleg S. 1997. Differential interaction of 1α,25-dihydroxyvitamin D_3 analogues and their 20-*epi* homologues with the vitamin D receptor. J Biol Chem 272:3336–3345.

Malloy PJ, Eccleshall TR, Gross C, Van Maldergem L, Bouillon R, Feldman D. 1997. Hereditary vitamin D resistant rickets caused by a novel mutation in the vitamin D receptor that results in decreased affinity for hormone and cellular hyporesponsiveness. J Clin Invest 99:297–304.

Midland MM, Plumet J, Okamura WH. 1993. Effect of C20 stereochemistry on the conformational profile of the side chains of vitamin D analogs. Bioorg Med Chem Lett 3:1799–1804.

Nakajima S, Hsieh JC, Jurutka PW, Galligan MA, Haussler CA, Whitfield GK, Haussler MR. 1996. Examination of the potential functional role of conserved cysteine residues in the hormone binding domain of the human 1,25-dihydroxyvitamin D_3 receptor. J Biol Chem 271: 5143–5149.

Nolte RT, Wisely GB, Westin S, Cobb JE, Lambert MH, Kurokawa R, Rosenfeld MG, Willson TM, Glass CK, Milburn MV. 1998. Ligand binding and co-activator assembly of the peroxisome proliferator-activated receptor-gamma. Nature 395:137–143.

Norman AW, Okamura WH, Hammond MW, Bishop JE, Dormanen MC, Bouillon R, Van Baelen H, Ridal AL, Daane E, Khoury R, Farach-Carson MC. 1997. Comparison of 6-s-*cis* and 6-s-*trans* locked analogs of 1α,25$(OH)_2$-vitamin D_3 indicates that the 6-s-*cis* conformation is preferred for rapid nongenomic biological responses and that neither 6-s-*cis* nor 6-s-*trans* locked analogs are preferred for genomic biological responses. Mol Endocrin 11:1518–1531.

Okamura WH, Palenzuela JA, Plumet J, Midland MM. 1992. Vitamin D: structure-function analyses and the design of analogs. J Cell Biochem 49:10–18.

Peleg S, Sastry M, Collins ED, Bishop JE, Norman AW. 1995. Distinct conformational changes induced by 20-epi analogues of 1α,25-dihydroxyvitamin D_3 are associated with enhanced activation of the vitamin D receptor. J Biol Chem 270:10551–10558.

Rachez C, Suldan Z, Ward J, Chang CP, Burakov D, Erdjument-Bromage H, Tempst P, Freedman LP. 1998. A novel protein complex that interacts with the vitamin D_3 receptor in a ligand-dependent manner and enhances VDR transactivation in a cell-free system. Genes Dev 12:1787–1800.

Raynaud J-P, Ojasoo T, Mornon J-P. 1991. Modeling the hormone-binding domain of steroid receptors including the vitamin D_3 receptor. In: Norman AW, Bouillon R, Thomasset M, editors. Vitamin D: Gene regulation, structure-function analysis and clinical application. Berlin: Walter de Gruyter. p 64–74.

Renaud J-P, Rochel N, Ruff M, Vivat V, Chambon P, Gronemeyer H, Moras D. 1995. Crystal structure of the RAR-γ ligand-binding domain bound to all-trans retinoic acid. Nature 378:681–689.

Ritchie HH, Hughes MR, Thompson ET, Malloy PJ, Hochberg Z, Feldman D, Pike JW, O'Malley BW. 1989. An ochre mutation in the vitamin D receptor gene causes hereditary 1,25-dihydroxyvitamin D_3-resistant rickets in three families. Proc Natl Acad Sci USA 86:9783–9787.

Tanenbaum DM, Wang Y, Williams SP, Sigler PB. 1998. Crystallographic comparison of the estrogen and progesterone receptor's ligand binding domains. Proc Natl Acad Sci USA 95:5998–6003.

Thompson E, Kristjansson K, Hughes MR. 1991. Molecular scanning methods for mutation detection: application to the 1,25-dihydroxyvitamin D receptor. Eighth Workshop on vitamin D: Abstract book 6.

Uskokovic M, Manchand PS, Peleg S, Norman AW. 1997. Synthesis and preliminary evaluation of the biological properties of a 1α,25-dihydroxyvitamin D_3 analog with two side-chains. In: Norman AW, Bouillon R, Thomasset M, editors. Vitamin D: chemistry, biology and clinical applications of the steroid hormone. Riverside, CA: University of California-Riverside Printing & Reprographics, pp 19–23.

Wagner RL, Apriletti JW, McGrath ME, West BL, Baxter JD, Fletterick RJ. 1995. A structural role for hormone in the thyroid hormone receptor. Nature 378:690–697.

Whitfield GK, Hsieh JC, Nakajima S, MacDonald PN, Thompson PD, Jurutka PW, Haussler CA, Haussler MR. 1995. A highly conserved region in the hormone-binding domain of the human vitamin D receptor contains residues vital for heterodimerization with retinoid X receptor and for transcriptional activation. Mol Endocrinol 9:1166–1179.

Whitfield GK, Selznick SH, Haussler CA, Hsieh JC, Galligan MA, Jurutka PW, Thompson PD, Lee SM, Zerwekh JE, Haussler MR. 1996. Vitamin D receptors from patients with resistance to 1,25-dihydroxyvitamin D_3: Point mutations confer reduced transactivation in response to ligand and impaire dinteraction with the retinoid X receptor heterodimeric partner. Mol Endocrinol 10:1617–1631.

Williams SP, Sigler PB. 1998. Atomic structure of progesterone complexed with its receptor. Nature 393:392–396.

Wurtz J-M, Guillot B, Moras D. 1997. 3D model of the ligand binding domain of the vitamin D nuclear receptor based on the crystal structure of holo RARγ. In: Norman AW, Bouillon R, Thomasset M, editors. Vitamin D: chemistry, biology and clinical applications of the steroid hormone. Riverside, CA: University of California-Riverside Printing and Reprographics, pp 165–172.

Wurtz J-M, Bourguet W, Renaud J-P, Chambon P, Moras D, Gronemeyer H. 1996. A canonical structure for the ligand-binding domain of nuclear receptors. Nature Struct Biol 3:87–94.

Yamada S, Yamamoto K, Masuno H, Ohta M. 1998. Conformation-function relationship of vitamin D: conformational analysis predicts potential side-chain structure. J Med Chem 41:1467–1475.